MODELLING OF RADIATION EXPOSURE AT HIGH-ALTITUDES DURING SOLAR STORMS

H. Al Anid[1], B.J. Lewis[1], L.G.I. Bennett[1] and M. Takada[2]

[1]Department of Chemistry and Chemical Engineering, Royal Military College of Canada,
P.O. Box 17000, Kingston, Ontario, K7K 7B4, Canada

[2] National Institute of Radiological Science, International Space Radiation Laboratory,
4-9-1, Anagawa, Inage-Ku, Chiba, 263-8555, Japan

Abstract

A transport code analysis using Monte Carlo N-Particle eXtended code, MCNPX, has been used to propagate an extrapolated particle spectrum based on satellite measurements through the atmosphere to estimate radiation exposure during solar storms at high altitudes. Neutron monitor count rate data from stations around the world were used to benchmark the model calculations during a Ground Level Event. A comparison was made between the model predictions and actual flight measurements taken with various types of instruments used to measure the mixed radiation field during GLE 60. A computer-code has been developed to implement the model for routine analysis.

1. Introduction

In 1990, the International Commission on Radiological Protection (ICRP) recognized the occupational exposure of aircrew to cosmic radiation[1]. In Canada, a Commercial and Business Aviation Advisory Circular (CBAAC) was issued by Transport Canada suggesting that action should be taken to manage such exposure[2]. In anticipation of possible regulations on exposure of Canadian-based aircrew in the near future, an extensive study was carried out at the Royal Military College of Canada (RMC) to measure the radiation exposure during flights.

The radiation exposure to aircrew is a result of a complex mixed-radiation field resulting from *Galactic Cosmic Rays* (GCRs) and *Solar Energetic Particles* (SEPs). Supernova explosions and active galactic nuclei are responsible for GCRs which consist of 90% protons, 9% alpha particles, and 1% heavy nuclei[3]. While they have a fairly constant fluence rate, their interaction with the solar magnetic field of the Earth varies throughout the solar cycles, which has a period of approximately 11 years. The radiation dose absorbed on airplanes due to GCR has been thoroughly studied and the empirical-based PCAire code developed at RMC can predict the radiation dose with good accuracy.

SEPs are highly sporadic events that are associated with solar flares and coronal mass ejections. While contributing less than 1% to the overall career exposure, this type of exposure may be of concern to certain aircrew members, such as pregnant flight crew, where the annual effective dose is limited to 1 mSv over the remainder of the pregnancy[4]. The composition of SEPs is very similar to GCRs, in that they consist of mostly protons, some alpha particles and a few heavy nuclei, but with a softer energy spectrum.

To estimate the additional exposure due to solar flares, a model was developed using a Monte-Carlo radiation transport code, MCNPX. The model transports an extrapolated flux spectrum through the atmosphere using the MCNPX analysis. This code produces the estimated flux at a specific altitude where ICRP conversion coefficients are applied to convert the particle flux into an ambient dose equivalent. Transporting the flux through the atmosphere to ground level enables calculations of expected neutron-monitor count rates, which can be compared against neutron monitor (NM) data obtained from stations around the world. A cut-off rigidity model accounts for the shielding effects of the Earth's magnetic field.

2. Model Development

2.1 Solar Flare Particle Spectrum

The particle spectrum resulting from a solar flare is highly variable and sporadic. Satellite measurements provide near real-time data. One specific instrument is the Space Environment Monitor (SEM) on the Geostationary Operational Environmental Satellites (GOES). The SEM is capable of measuring the flux of solar and galactic particles and X-rays. The proton flux measurements necessary for our model are provided by energetic particle sensors (EPS) and the high-energy proton and alpha detector (HEPAD), which operate over a large range of energies (Table 1).

In order to transport the particle spectrum through the atmosphere, the GOES measurements must be extrapolated to a high energy of 10 GeV, which is accomplished by fitting the GOES data to a power-law equation for the differential flux using:

$$\phi(E) = \frac{C}{\beta}\left(\frac{R}{R_o}\right)^{-\gamma} \quad \textbf{(1)}$$

where C and γ are fitting parameters. C is calculated using actual GOES measurements and γ is adjusted until the average variance between the extrapolated flux and the HEPAD measurements falls below 1%.

The particle rigidity R (in MV) is related to its energy E (in MeV) by the relation:

$$R = \sqrt{E\left(E + 2E_o\right)} \quad \textbf{(2)}$$

where E_o is the rest mass energy of the particle (in MeV) and $\beta = R/\left(R^2 + E_o^2\right)^{1/2}$ is the particle velocity v normalized by the speed of light c. The parameter R_o = 239 MV in **(1)** corresponds to a particle energy of E = 30 MeV.

An example of the extrapolated spectrum using satellite data is shown in Figure 1.

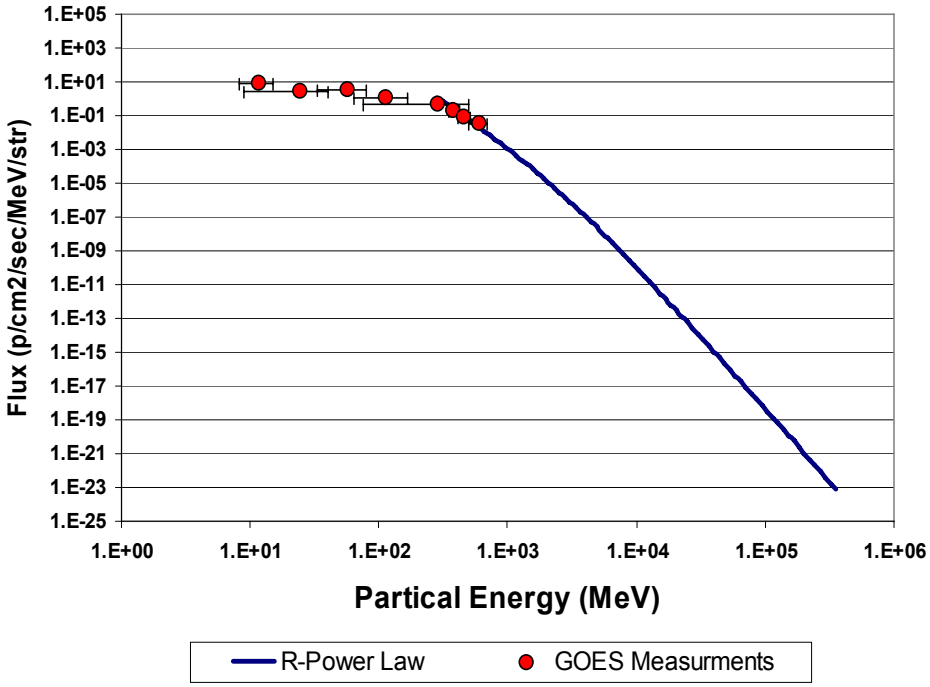

Figure 1 High-Energy extrapolation of differential proton energy data from the GOES satellite for GLE 60.

2.2 MCNPX Analysis

A Monte Carlo simulation refers to any simulation process in which there is a stochastic or random element, normally expressed in a simulation algorithm through the use of random numbers. Since particle physics models are very complex, it may be very difficult or even impossible to solve exactly for the properties of the system. A Monte Carlo simulation can be used for such models as a method for iteratively solving the problem of radiation transport.

Monte Carlo N-Particle eXtended code, MCNPX, is a 3-Dimensional Monte Carlo radiation transport code developed by the Los Alamos National Laboratory. The code is capable of tracking 34 particle types (nucleons and light ions) and 2000+ heavy ions at nearly all energies. It uses standard evaluated data libraries including physical-based models where data libraries are not yet available.

The MCNPX code (version 2.5) was used to determine the particle production and transport in the atmosphere. Although secondary particles are produced by interaction of primary cosmic ray particles with atmospheric nuclei, only the production of neutrons and protons were considered. The atmosphere was divided into 36 concentric shells using an average air density for a given shell thickness. Secondary particle energy spectra produced from an incident mono-energetic source particle was tracked in the analysis[5]. Combined particle spectra (at a given altitude) were therefore obtained by summing the secondary particle spectra derived from each mono-energetic primary particle based on the initial proton spectrum and helium spectrum. Dose conversion factors as well as neutron monitor response functions have been incorporated with the MCNPX results for a specific altitude[6].

As a preliminary test, the interstellar GCR spectrum was used to predict neutron and proton spectra on the ground and at 17 km. These results were compared to those measured by Goldhagen and Gordon and were determined to be in reasonable agreement. [7-9] Further comparisons were made with measured neutron Bonner-sphere results for various altitudes and vertical cut-off rigidities (Figure 2).

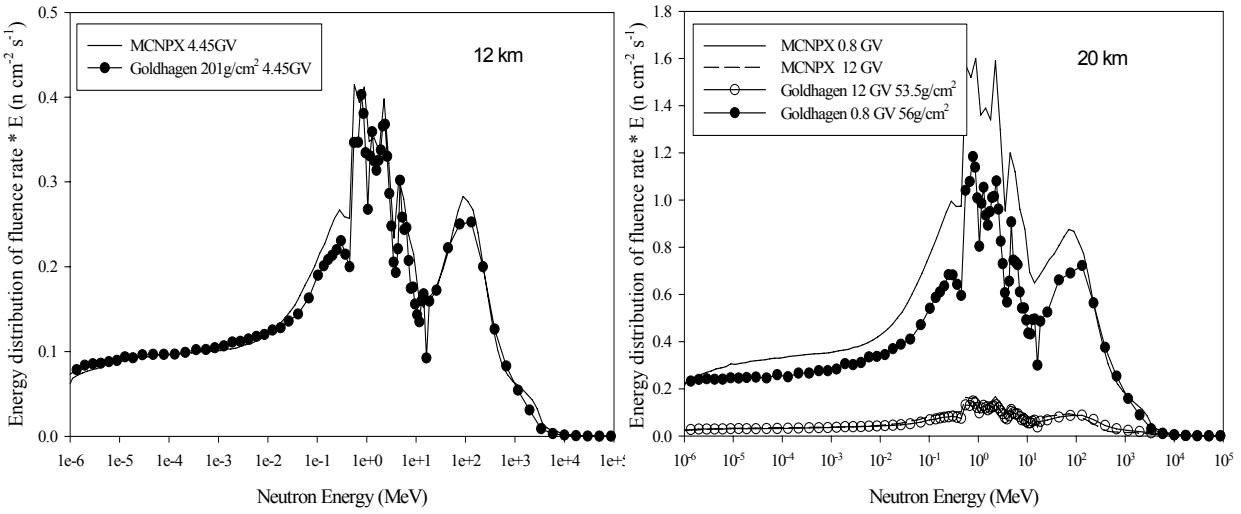

Figure 2 Comparison of predicted and measured neutron spectra at various altitudes and vertical cut-off rigidities.

Based on this agreement, the MCNPX analysis was applied to the SEP particle spectrum. For the GCR spectrum, a spherical geometry was used, since galactic rays are assumed to be isotropic, arriving from any direction. For the solar flare code, a planer source geometry was used. Figure 3 illustrates both geometries for transporting particles through the Earth's atmosphere.

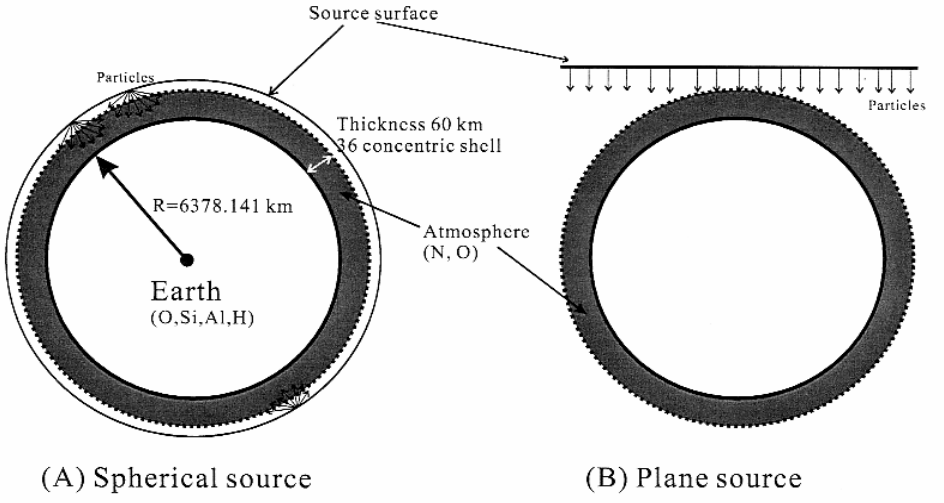

Figure 3 Spherical and Planer geometry for MCNPX transport code

The coefficients obtained from the MCNPX analysis, P_{ij}, are combined with dose conversion coefficients, K_j, and NM response functions, R_j, using equations **(3)** and **(4)**. Different coefficients are used for ambient dose equivalent rate ($\dot{H}$) and effective dose rate ($\dot{E}$) for equation **(3)**, while different NM detector type response functions are used in equation **(4)**. A complete list of tabulated P_A and P_{NM} coefficients are given in Reference 6.

$$\dot{E}, \dot{H}(\mathrm{Sv\ h^{-1}}) = \sum_{i=1}^{m}\left[\sum_{j=1}^{n}\left\{c\cdot\Delta E_{i,i+1}\cdot K_j\cdot P_{ij}\cdot\left(\frac{3600\ \mathrm{s}}{\mathrm{h}}\right)\right\}\dot{\Phi}_{E,\Omega_i}^{prim}\right] = \sum_{i=1}^{m} P_A(E_i)\,\dot{\Phi}_{E,\Omega}^{prim}(E_i) \quad \textbf{(3)}$$

$$\dot{C}(\mathrm{count\ h^{-1}}) = \sum_{i=1}^{m}\left[\sum_{j=1}^{n}\left\{c\cdot\Delta E_{i,i+1}\cdot R_j\cdot P_{ij}\cdot\left(\frac{3600\,s}{h}\right)\right\}\dot{\Phi}_{E,\Omega_i}^{prim}\right] = \sum_{i=1}^{m} P_{NM}(E_i)\,\dot{\Phi}_{E,\Omega}^{prim}(E_i) \quad \textbf{(4)}$$

2.3 Vertical Cut-off Rigidity

The Earth's magnetic field acts as a shield to incoming particles and radiation. Particles that do not have sufficient energy to penetrate the Earth's field are reflected back into space. Therefore, a model of the cutoff rigidity has to take into account the properties of the Earth's magnetic field as well as geographical position.

During an SPE, the Earth is bombarded with energetic particles causing major disturbances in the field. Not only do the particles contribute largely to the already-existing radiation (due to GCR), the solar wind during a geomagnetic storm can perturb the Earth's magnetic field thus lowering the cutoff rigidity.

The cut-off rigidity model used in our analysis is a value obtained by averaging a quiet sun model, R_U, and a noisy sun model, R_L. The quiet sun model uses the vertical cut-off rigidity, R_C (in GV) obtained from standard International Geomagnetic Reference Field (IGRF) maps (1995 model), while the noisy sun model is calculated using[10]:

$$R_L(GV) = \left\{1 - 0.54\exp\left(-R_c(GV)/2.9\right)\right\} \quad \textbf{(5)}$$

The effect of the cutoff rigidity is taken into consideration in the calculation by summing up only those particles with energies greater than the corresponding energy for a given vertical cutoff rigidity, R_c (using Eq. 2). A low pass energy filter was applied to match the NM data where primary protons with energy less than 430 MeV were ignored in the summation. This filter was chosen by matching predicted results to observed ground-level NM data (see Table 2 for NM characteristics). This filter accounts for the ability of lower energy particles to reach the neutron monitor at ground level.

Figure 4 illustrates the prediction of the model using various cutoff filters, leading to the final choice of 1 GV. Figure 5 shows a comparison between the predicted NM count rates against data from NM stations around the world for Ground Level Event (GLE) 60.

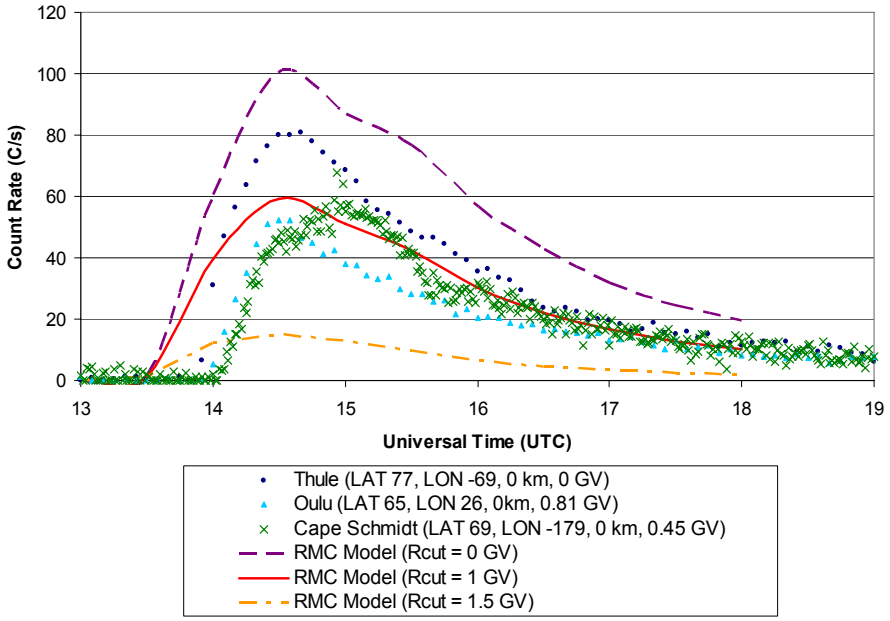

Figure 4 Observed count rate history (minus background GCR) versus model predictions for GLE 60 (April 15th, 2001)

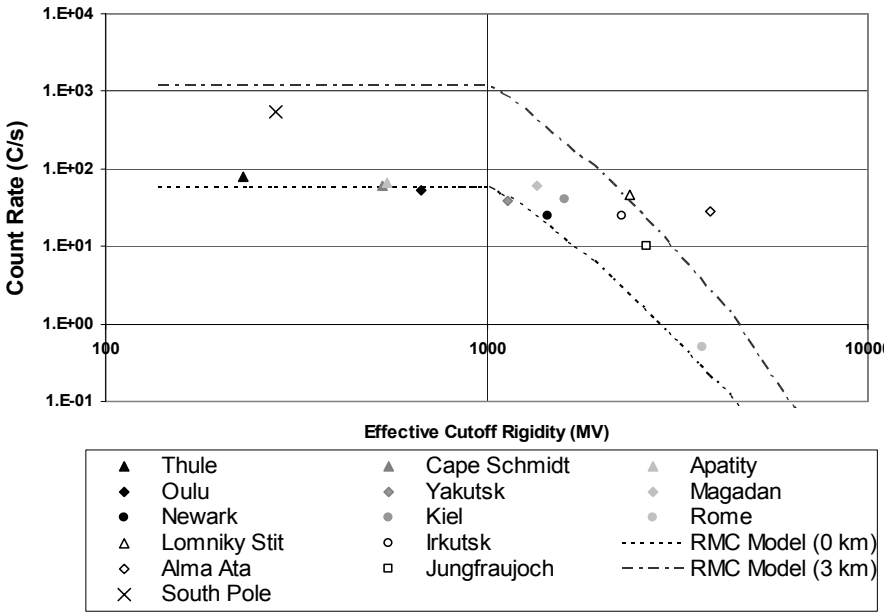

Figure 5 Comparison of the model calculations to the observed peak count rates for various NMs located around the world during GLE 60. (Hollow shapes represent NMs at an altitude of 3 km and solids represent NMs at an altitude of 0 km)

3. Software Development

To perform the calculation on a routine basis, a computer code was developed using C++. The code, compiled as a Dynamically Linked Library (DLL), includes several modules that perform all the necessary input data acquisition and great circle route calculations, as well as the analysis required for estimating the radiation dose absorbed by aircrew at a given altitude.

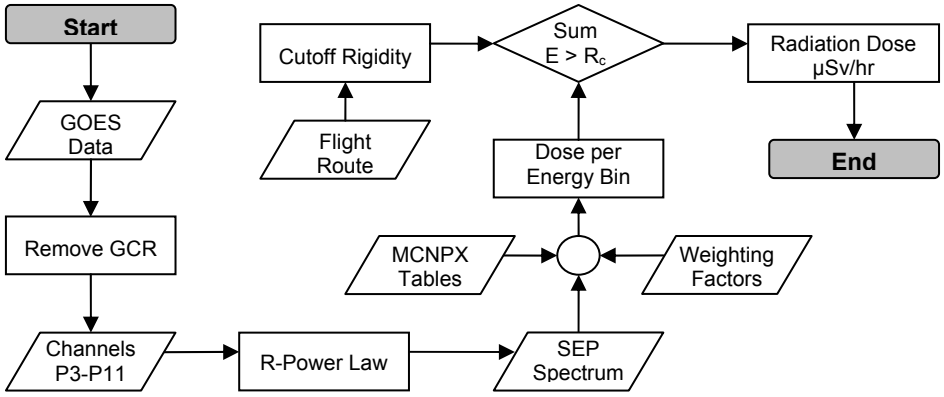

Figure 6 Flowchart describing the general methodology for calculating the radiation dose.

To simplify the end-user experience, a Graphical User Interface (GUI) was developed using Visual Basic that calls the DLL calculation routine. The GUI allows the user to enter flight data either in "Flight Information" mode or in "Waypoint" mode. In the former, the user provides the departure and arrival airports, and a great circle route calculator estimates the flight route. In the latter, the user provides a list of waypoints each containing latitude, longitude, and altitude information for the actual flight route. Figure 7 shows an image of the user interface running in "Flight Information" mode.

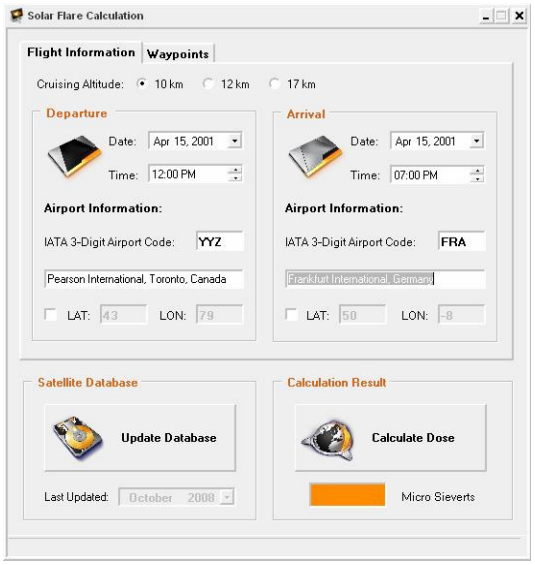

Figure 7 The graphical user interface used for implementing the solar flare calculation.

4. Results and Analysis

To test the validity of the model, it was necessary to perform the solar flare calculation on GLEs where actual flight measurements exist, allowing direct comparison. One such event is GLE 60, where flight measurements were taken as part of the EU DOSMAX (Dosimetry of Aircrew Exposure during Solar Maximum) project. One flight from Prague to New York (PRG-JFK) employed a MDU-Liulin device[11], whereas a second flight from Frankfurt to Dallas Fort Worth (FRA-DFW) used an ACREM monitor (scaled GM tube measurements) for radiation monitoring[12].

To calculate the SEP exposure, the initial proton fluence rates were first obtained by subtracting the GCR component from the GOES measurement. Here, the GCR component was obtained from spectra that were averaged prior to the event. The GCR exposure was estimated from the PCAire code and summed with the SEP estimate to obtain a total determination of the aircrew exposure.

The results are illustrated in Figures 8 and 9. Good agreement is observed with a discrepancy between the model and measurements of typically less than ±25%. As seen in the figure, the solar flare contributed 45% to the total cumulative dose of 54 μSv for the PRG-JFK route.

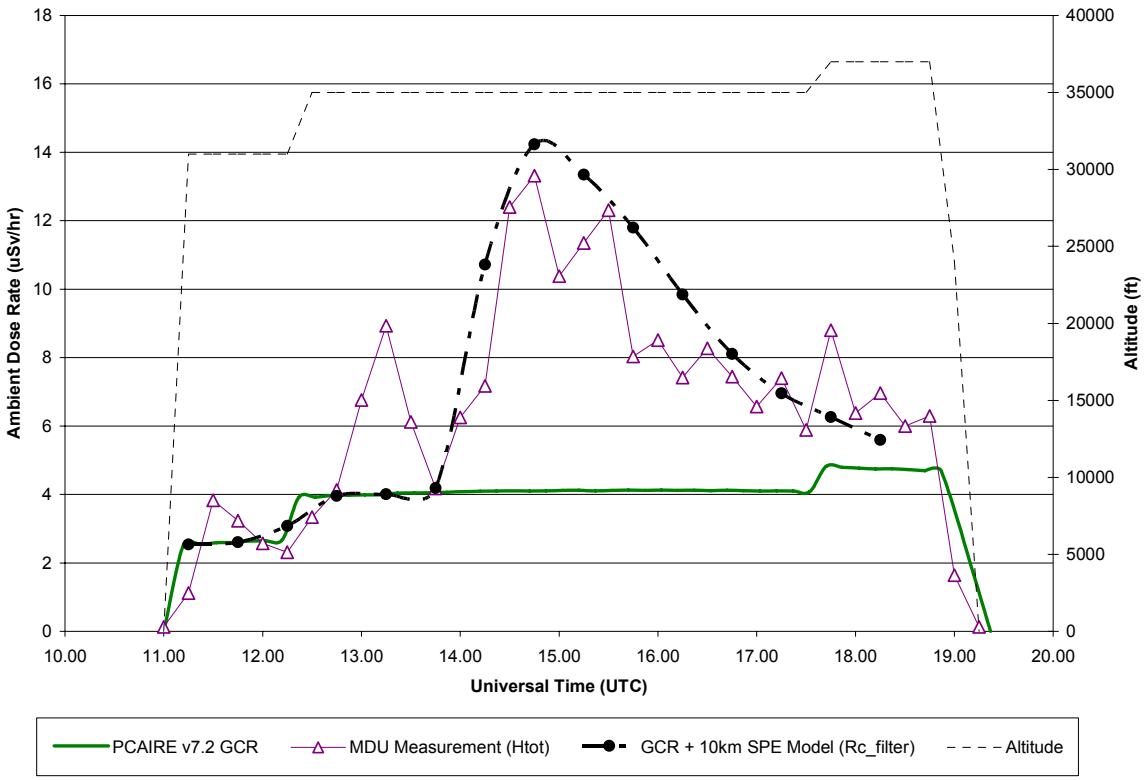

Figures 8 Comparison of calculations and measurements of the ambient dose equivalent rates during GLE 60 for PRG-JFK flight

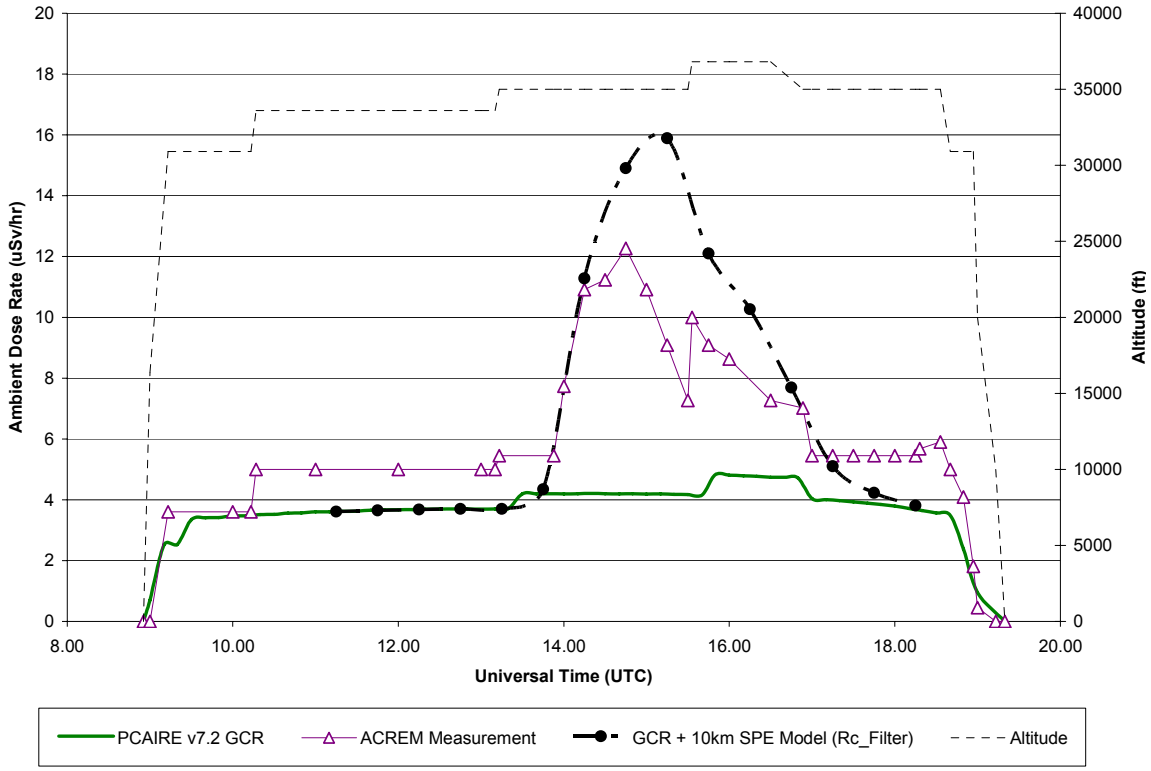

Figures 9 Comparison of calculations and measurements of the ambient dose equivalent rates during GLE 60 for FRA-DFW flight

5. Summary and Conclusions

A transport code analysis with MCNPX is used to propagate an extrapolated particle spectrum based on satellite measurements through the atmosphere in order to estimate additional aircrew exposure from the SEP event. The transport code calculation is benchmarked against actual neutron spectra measured at high altitudes and on the ground. A routine methodology has been developed to estimate the aircrew exposure for the SEP contribution. These computations are compared with count rate data observed at various NMs on the ground as well as ambient dose equivalent rate measurements made on-board jet aircraft during GLE 60.

6. References

[1] International Commission on Radiological Protection, *1990 Recommendations of the International Commission on Radiological Protection*, ICRP Publication 60, Pergamon Press, Oxford (1991).

[2] Transport Canada, "Measures for Managing Exposure to Cosmic Radiation of Employees Working On Board Aircraft," Commercial and Business Aviation Advisory Circular No. 0183 (2001).

[3] W. Heinrich, S. Roesler and H. Schraube, "Physics of Cosmic Radiation Fields," *Radiation Protection Dosimetry*, **86**(4), 253-258 (1999).

[4] B.J. Lewis, M. Desormeaux, A.R. Green, L.G. I. Bennett, A. Butler, M. McCall and J.C. Saez Vergara, "Assessment of Aircrew Radiation Exposure by Further Measurements and Model Development," *Radiation Protection Dosimetry,* **111**(2), 151-171 (2004).

[5] International Organization for Standardization, "Probabilistic model for particle fluences and peak fluxes of solar energetic particles," ISO TS 15391, October 2004.

[6] M. Takada, B.J. Lewis, M. Boudreau, H. Al Anid, and L.G.I Bennet, "Modeling of Aircrew Radiation Exposure from Galactic Cosmic Rays and Solar Particle Events", *Radiation Protection Dosimetry*, DOI: 10.1093/RPD/NCM214 (2007)

[7] J.M. Clem, G. De Angelis, P. Goldhagen and J.W. Wilson, *Radiation Protection Dosimetry*, 110(1/4), 423 (2004).

[8] M.S. Gordon, P. Goldhagen, K.P. Rodbell, T.H. Zabel, H.H.K. Tang, J.M. Clem and P. Bailey, *IEEE Transactions on Nuclear Science*, 51(6), 3427 (2004).

[9] P. Goldhagen, J.M. Clem, and J.W. Wilson, *Advances in Space Research*, 32(1), 35 (2003).

[10] The Space Environment Information System, Background Information in SPENVIS; Single event upsets. www.spenvis.oma.be/spenvis/help.html. Date accessed: Sept. 2005.

[11] F. Spurny and T. Dachev. "Intense solar flare measurements", *Radiation Protection Dosimetry*. **95**, 273-275 (2001).

[12] D.T. Bartlett *et al.* "Investigation of radiation doses at aircraft altitudes during a complete solar cycle", SOLSPSA Space Weather Workshop, Vico Equense, Italy, September 25-29, (2001).

Table 1: Energy channels for Protons, Alphas and Electrons for the GOES-11 Satellite (EPS and HEPAD)

Particle Type	Channel number	Energy range (MeV)	Detector Assembly	Particle Rigidity (MV)
Proton	P1	0.8 - 4	Telescope	
	P2	4 - 9	Telescope	
	P3	9 - 15	Telescope	168 – 130
	P4	15 - 40	Dome	277 – 168
	P5	40 - 80	Dome	396 – 277
	P6	80 - 165	Dome	580 – 396
	P7	165 - 500	Dome	1090 – 580
	P8	350 - 420	HEPAD	982 – 883
	P9	420 - 510	HEPAD	1103 –982
	P10	510 - 700	HEPAD	1343 – 1103
	P11	≥700	HEPAD	
Alpha	A1	4 – 10	Telescope	
	A2	10 – 21	Telescope	
	A3	21 – 60	Telescope	
	A4	60 – 150	Dome	
	A5	150 – 250	Dome	
	A6	300 – 500	Dome	
	A7	2560 – 3400	HEPAD	
	A8	≥3400	HEPAD	
Electron	E1	≥0.6	Dome	
	E2	≥2.0	Dome	
	E3	≥4.0	Dome	

Table 2: Details of Ground-Based Neutron Monitors around the World

Station	Latitude (deg)	Longitude (deg)	Altitude (m)	Air Depth (g cm^{-2})	Detector Type	Vertical Cut-off Rigidity (GV)
Alma-ata	43.25	76.92	3340	675	18NM64	6.61
Apatity	67.55	33.33	177	1000	18NM64	0.57
Athens	37.98	23.78	260	980	6NM64	8.53
Baksan	43.28	42.69	1700	820	6NM64	5.6
Barensburg	78.12	14.42	0	1000	6NM64	0.05
Calgary	51.08	-114.13	1128	883	12NM64	1.08
Cape Shmidt	68.55	180.32	0	1016	12NM64	0.45
Climax	39.37	-106.18	3400	672	IGY	2.99
Erevan	40.5	44.17	3250	700	18NM64	7.58
Fort-Smith	60	-112	0	1013.3	18NM64	0
Haleaka	20.72	-156.27	3052	830	18NM64	13.3
Herman	-34.42	19.23	26	1035	12NM64	4.58
Inuvik	68.35	-133.72	21	1033.3	18NM64	0.17
Irkustk	52.47	104.03	435	984	18NM64	3.64
Jungraujoch	46.55	7.98	3475	655.7	3NM64	4.54
Kerguelen	-49.35	70.27	33	1019.7	IGY	1.14
Kiel	54.3	10.1	54	1026.5	18NM64	2.36
Larc	-62.2	-58.96	40	999.3	6NM64	3
Lomnicky	49.2	20.22	2634	761.7	IGY	3.98
McMurdo	-77.9	166.6	48	992.5	18NM64	0
Moscow	55.47	37.32	200	1019.7	24NM64	2.43
Mawson-Antractica	-67.6	62.88	0	1009.52	18NM64	0.22
Mexico	19.33	-99.2	2274	794.4	6NM64	9.53
Nain	56.6	-61.7	0	1033.3	18NM64	0
Norilsk	69.26	88.05	0	1024.8	18NM64	0.58
Novosibirsk	54.48	83	163	1014.6	24NM64	0.58
Newark	39.7	-75.7	50	1033.3	9NM64	2.87
Oulu	65.06	25.47	0	1019.7	9NM64	2.09
Peawanuck	55	-85	0	1033.3	18NM64	7
Rome	41.9	12.52	60	1028.9	17NM64	6.32
Sanae	-71.67	-2.85	856	897.4	6NM64	0.86
South Pole	-90	0	2820	693.4	3NM64	0.09
Tbilisi	41.43	44.48	510	984	18NM64	6.73
Terre Adelie	-66.67	140.02	45	1006.5	9NM64	0.02
Thule-Greenland	76.6	-68.8	260	1025.1	9NM64	0
Tsumeb	-19.2	17.58	1240	897.4	18NM64	9.21
Tixie	71.36	128.54	0	1019.7	18NM64	0.48
Yakutsk	62.01	129.43	105	1019.7	18NM64	1.65